A new charge density wave oxide, $LiVMoO_5$, and its tungsten analogue obtained by topotactic reduction of $LiVMO_6$ (M = Mo, W) brannerites†

J. Gopalakrishnan,* N. S. P. Bhuvanesh, R. Vijayaraghavan and N. Y. Vasanthacharya

Solid State and Structural Chemistry Unit, Indian Institute of Science, Bangalore-560 012, India

We report the synthesis of two new low-dimensional oxides, $LiVMO_5$ (M = Mo, W), which contain $S = \frac{1}{2}$ transition-metal atoms, $V^{IV}: 3d^1$ and $Mo^V: 4d^1/W^V: 5d^1$, by topotactic reduction of the $LiVMO_6$ brannerites in hydrogen. $LiVMO_5$ crystallizes in orthorhombic structures related to the parent brannerite structure. The VMO_5 network of the new oxides is likely to correspond to one of the A_2X_5 structures predicted by A. F. Wells (*Philos. Trans. R. Soc. London A*, 1984, **312**, 589). $LiVMoO_5$ is metallic showing a charge density wave (CDW) instability around 230 K; interestingly, $LiVWO_5$ is a paramagnetic semiconductor down to 20 K.

Several transition-metal oxides containing $S = \frac{1}{2}$ metal atoms exhibit novel electronic properties, especially when the electronic interaction is not uniform in all the three dimensions. For example, rutile-like VO_2 shows a metal–insulator transition[1–3] at 340 K that is accompanied by cell doubling, pairing of V atoms and charge ordering; quasi-low-dimensional molybdenum oxides $A_xMo_6O_{17}$ (A = Na, K, Tl) and Mo_4O_{11} containing $S = \frac{1}{2}$ Mo^V are two-dimensional (2D) metals showing charge density wave (CDW) instabilities[4,5] at low temperatures; $S = \frac{1}{2}$ spin-ladder compounds‡ such as $SrCu_2O_3$, $Sr_2Cu_3O_5$, $LaCuO_{2.5}$ and $(VO)_2P_2O_7$ show short- and long-range spin correlations that depend on whether the ladder legs are even or odd;[6] and, last but not least, La_2CuO_4 is a well known $S = \frac{1}{2}$ 2D antiferromagnet that shows superconductivity[7,8] when appropriately doped with holes.

All these oxides contain only one kind of $S = \frac{1}{2}$ metal atom, namely V^{IV}, Mo^V or Cu^{II}. We considered it interesting to synthesize new low-dimensional transition-metal oxides containing two different $S = \frac{1}{2}$ metal atoms and explore the electronic properties. Here we report the synthesis of two such oxides, $LiVMO_5$ (M = Mo, W) containing $V^{IV}: 3d^1$ and $Mo^V: 4d^1/W^V: 5d^1$, and the characterization of their structure and electronic properties. The synthesis of these oxides was achieved by a topochemical reduction of the well known layered oxides,[9,10] $LiVMO_6$ (M = Mo, W), possessing the brannerite structure.[11] The electronic properties of these oxides reveal that while the tungsten compound, $LiVWO_5$, is a paramagnetic insulator down to 20 K, the molybdenum analogue, $LiVMoO_{5.04}$, is a metal showing indications of a CDW instability below 230 K. We believe that this is the first report of a CDW transition in a metal oxide containing two different $S = \frac{1}{2}$ transition-metal atoms.

Experimental

$LiVMO_6$ (M = Mo, W) was prepared, as reported in the literature,[9,10] by reacting Li_2CO_3 and V_2O_5 first at 550 °C for 24 h to give $LiVO_3$, which was heated subsequently with MoO_3 (at 550 °C) or WO_3 (at 650 °C) for 24 h. Reduction of $LiVMO_6$ was investigated by thermogravimetry (TG; Cahn TG-131 system) at a heating rate of 2 °C min^{-1}, under flowing hydrogen diluted with nitrogen (H_2–N_2 in the ratio 1 : 2). From the TG results (Fig. 1), we determined that bulk $LiVMO_5$ could be prepared by reducing pellets of $LiVMO_6$ (at 560 °C for M = Mo and at 575 °C for M = W) in dilute hydrogen (H_2–N_2 in the ratio 1 : 2) for 2 h with one intermittent grinding and pelleting.

The parent oxides, $LiVMO_6$, and their reduced products, $LiVMO_5$, were characterized by X-ray powder diffraction (XRD; JEOL JDX-8P X-ray powder diffractometer; Cu-Kα radiation). Unit-cell parameters were derived by least-squares refinement of the powder diffraction data using the PROSZKI program.[12] The oxygen stoichiometry/oxidation state of transition-metal atoms in $LiVMO_5$ was determined by redox potentiometric titration using Ce^{4+} as the oxidant. The mass gain during reoxidation of the samples in the TG balance provided an additional check of the oxygen stoichiometry. The powder XRD pattern of the oxidized material coincided with that of the parent $LiVMO_6$.

Electrical resistivity measurements of $LiVMO_5$ were carried out on as-prepared pellets by a four-probe technique in the temperature range 300–20 K using a closed cycle helium cryostat. Dc magnetic susceptibility measurements were made in the 300–20 K range using a Lewis Coil magnetometer (George Associates, USA, Model 2000).

Results and Discussion

$LiVMO_6$ (M = Mo, W)[9,10] crystallizes in the brannerite ($ThTi_2O_6$) structure[11] (Fig. 2) which consists of edge- and corner-sharing $M'O_6$ (M′ = transition metal) octahedra. The

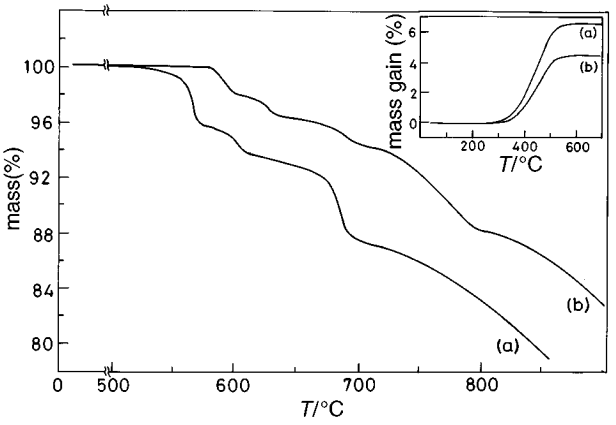

Fig. 1 Thermogravimetry (TG) curves for the reduction of (a) $LiVMoO_6$ and (b) $LiVWO_6$. The inset shows the TG curves for the reoxidation of (a) $LiVMoO_{5.04}$ and (b) $LiVWO_5$.

† Contribution No. 1231 from the Solid State and Structural Chemistry Unit.

‡ Spin-ladder compounds contain two or more metal–oxygen–metal chains interconnected by oxygen atoms.

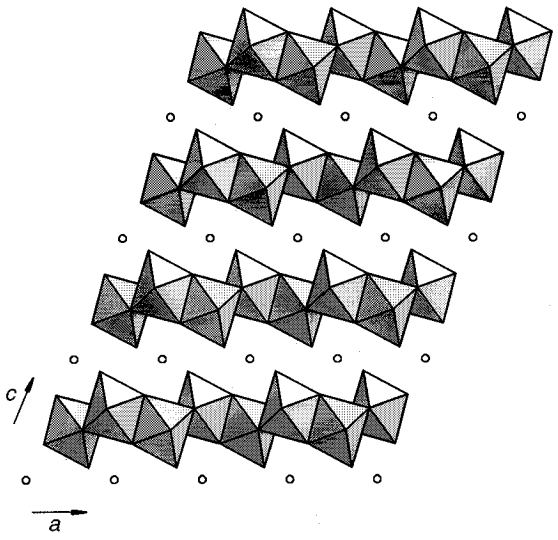

Fig. 2 Polyhedral view of the brannerite structure of $LiVMO_6$. Open circles in the interlayer space represent the Li atoms. The structure is drawn from the atomic positional parameters of $LiVWO_6$ given in ref. 10, using ATOMS software.

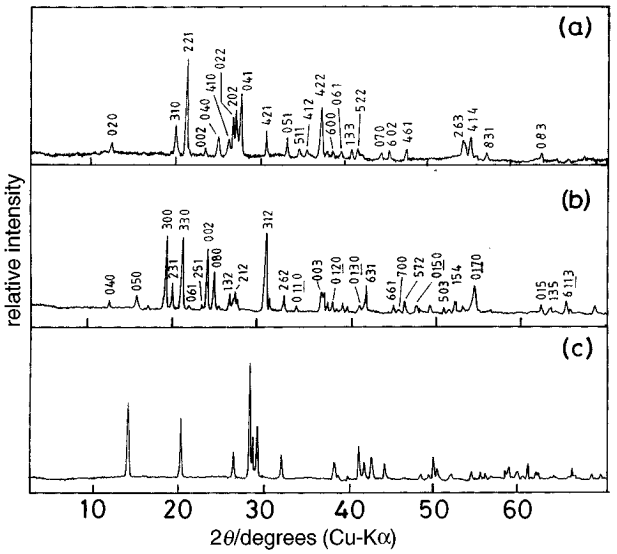

Fig. 3 X-Ray powder diffraction patterns of (a) $LiVMoO_{5.04}$ and (b) $LiVWO_5$. (c) XRD pattern of the oxidation product of $LiVMoO_{5.04}$. This pattern coincides with that of $LiVMoO_6$.

Table 1 Composition, lattice parameters, CDW transition temperature (T_c) and room-temperature resistivity (ρ_{RT}) of $LiVMO_5$

	lattice parameters/Å				
composition	*a*	*b*	*c*	T_c/K	ρ_{RT}/Ω cm
$LiVMoO_{5.04}$	14.122(1)	14.328(2)	7.618(1)	230	0.052
$LiVMoO_{5.08}$	14.143(7)	14.578(9)	7.587(3)	240	0.096
$LiVWO_5$	14.06(2)	28.81(1)	7.466(3)	—	58

connectivity of the octahedra could be represented as $M'O_{1/1}O_{2/2}O_{3/3}$, indicating that one of the oxygen atoms of each octahedron is unshared. The negative charges on the M'_2O_6 sheets are compensated by additional cations (Li or Th) which reside in the interlayer space.

The M'_2O_6 sheets of the brannerite structure could be visualized to give rise to a new M'_2O_5 framework by sharing the unshared oxygens. The connectivity of this new framework would be $M'O_{3/2}O_{3/3}$. The possibility of such an A_2X_5 structure derived from the brannerite was predicted by Wells in his classic paper surveying octahedral structures.[13]

We chose $LiVMO_6$ (M = Mo, W) for the realization of the new M'_2O_5 framework since both V^V and Mo^{VI}/W^{VI} can be reduced easily to V^{IV} and Mo^V/W^V by hydrogen at relatively low temperatures. Our TG studies† (Fig. 1) showed clearly the formation of an intermediate corresponding to the composition $LiVMO_5$. While the synthesis of bulk $LiVWO_5$ could be achieved readily by heating presintered pellets of $LiVWO_6$ at 575 °C for 2 h in flowing hydrogen diluted with nitrogen, the synthesis of stoichiometric $LiVMoO_5$ required careful monitoring of temperature and duration of reduction. For example, a sample of $LiVMoO_{5.04}$ was obtained by reduction at 560 °C for 2 h, whereas the composition of a sample obtained by reaction at 550 °C for 2 h was $LiVMoO_{5.08}$. The compositions, together with other characteristics of the $LiVMO_5$ phases synthesized, are given in Table 1. Since V^{IV} and Mo^V/W^V are the most likely oxidation states accessible under the experimental synthesis conditions, the reduced phases could be formulated as $LiV^{IV}M^VO_5$. Other combinations of oxidation states, *viz.* V^{III}, Mo^{VI}/W^{VI} and V^V, Mo^{IV}/W^{IV}, are unlikely on the basis of the redox characteristics of these transition metals.

The XRD pattern of $LiVMoO_5$ [Fig. 3(a)] could be indexed on an orthorhombic cell [$a = 14.122(1)$, $b = 14.328(2)$, $c = 7.618(1)$ Å; Table 2]. The pattern of $LiVWO_5$ [Fig. 3(b)] also indexes on a similar orthorhombic cell [$a = 14.06(2)$, $b = 28.81(1)$, $c = 7.466(3)$ Å; Table 3], but with a doubling of the *b* axis as compared to $LiVMoO_5$. On comparing the lattice parameters of the parent brannerite (for $LiVMoO_6$: $a = 9.347$, $b = 3.670$, $c = 6.632$ Å, $\beta = 111° 28'$) with the lattice parameters of $LiVMoO_5$, we see the following relationships: $a(LiVMoO_5) \approx \sqrt{2}a(LiVMoO_6)$, $c(LiVMoO_5) \approx 2b(LiVMoO_6)$.

The unshared vertex pointing towards the interlayer space [Fig. 4(a)], shares a similar vertex in the adjacent slab, thus eliminating an oxygen atom on reduction. Hence we expect a

Table 2 X-Ray powder diffraction data for $LiVMoO_5$[a]

h	*k*	*l*	d_{obs}/Å	d_{calc}/Å	I_{obs}
0	2	0	7.167	7.165	14
3	1	0	4.473	4.472	34
2	2	1	4.210	4.197	100
0	0	2	3.810	3.810	9
0	4	0	3.583	3.582	23
4	1	0	3.427	3.427	19
0	2	2	3.363	3.364	43
2	0	2	3.351	3.353	54
0	4	1	3.243	3.242	65
4	2	1	2.926	2.924	28
0	5	1	2.706	2.682	21
5	1	1	2.603	2.604	9
4	1	2	2.546	2.548	8
4	2	2	2.439	2.435	54
4	4	1	2.386	2.388	8
6	0	0	2.353	2.353	8
0	6	1	2.279	2.279	8
1	3	3	2.214	2.215	11
5	2	2	2.163	2.163	8
0	7	0	2.045	2.047	9
6	0	2	2.002	2.002	9
4	6	1	1.914	1.915	10
2	6	3	1.689	1.689	20
4	1	4	1.663	1.665	26
8	3	1	1.618	1.618	9
0	8	3	1.465	1.464	9

[a] $a = 14.122(1)$, $b = 14.328(2)$, $c = 7.618(1)$ Å.

† The TG curve of $LiVMoO_6$ (Fig. 1) shows three intermediate stages corresponding to the loss of 0.5, 1 and 2 oxygens, the final product of reduction being a mixture of $LiVO_2$ and MoO_2 at 700 °C. On the other hand, the TG curve of $LiVWO_6$ shows four stages corresponding to the loss of 0.5, 1, 1.25 and 2.5 oxygens up to 800 °C.

Table 3 X-Ray powder diffraction data for $LiVWO_5$[a]

h	k	l	d_{obs}/Å	d_{calc}/Å	I_{obs}
0	4	0	7.225	7.204	10
0	5	0	5.735	5.763	23
3	0	0	4.683	4.689	94
2	3	1	4.495	4.518	34
3	3	0	4.230	4.231	90
0	6	1	4.040	4.040	9
2	5	1	3.818	3.828	7
0	0	2	3.738	3.733	78
0	8	0	3.612	3.602	50
4	0	0	3.520	3.516	5
1	3	2	3.370	3.378	24
2	1	2	3.284	3.277	27
0	8	1	3.249	3.245	16
3	1	2	2.903	2.906	100
2	5	2	2.858	2.862	19
2	6	2	2.722	2.712	22
0	11	0	2.618	2.619	9
0	0	3	2.488	2.489	26
4	3	2	2.475	2.475	26
1	11	1	2.435	2.435	14
0	12	0	2.401	2.402	12
0	4	3	2.358	2.352	9
2	11	1	2.330	2.332	14
3	11	0	2.287	2.287	10
0	13	0	2.214	2.217	10
6	3	1	2.178	2.179	36
6	6	1	2.029	2.029	10
7	0	0	2.002	2.009	6
5	7	2	1.973	1.972	17
0	15	0	1.922	1.921	10
7	3	1	1.903	1.903	9
5	0	3	1.864	1.864	13
0	16	0	1.804	1.801	10
3	15	0	1.779	1.778	8
1	5	4	1.762	1.762	11
3	15	1	1.729	1.729	11
0	17	0	1.694	1.695	38
0	1	5	1.491	1.492	12
1	3	5	1.468	1.468	10
6	11	3	1.429	1.430	18

[a] $a = 14.06(2)$, $b = 28.81(1)$, $c = 7.466(3)$ Å.

decrease in the c parameter of $LiVMoO_6$; accordingly, we have $b(LiVMoO_5) < 3c(LiVMoO_6)$.

Also the reduction of $LiVMO_6$ and subsequent reoxidation of the product $LiVMO_5$ phases occur reversibly at relatively low temperatures (500–575 °C) suggesting that the $LiVMO_6$–$LiVMO_5$ transformation is most probably topotactic. Thus on the basis of lattice parameters and reversible reduction–oxidation, we propose a schematic model for the transformation of $LiVMoO_6$–$LiVMoO_5$ in Fig. 4. We see that the structure proposed for $LiVMoO_5$ in the *ab* plane is topologically similar to the structure of $LiVMoO_6$ in the *ac* plane, except that the unshared oxygens in the adjacent layers of the latter structure are connected to produce a quasi-two-dimensional structure in the former. Accordingly, the possible topotactic relationships are: [100](LiVMoO$_5$)‖[100](LiVMoO$_6$); [010](LiVMoO$_5$)‖[001](LiVMoO$_6$); [001](LiVMoO$_5$)‖[010](LiVMoO$_6$). We believe that similar topotactic relationships exist between $LiVWO_5$ and $LiVWO_6$.

From the connectivity of the metal–oxygen octahedra in the $LiVMoO_5$ structure [Fig. 4(b)], we see that the electronic interaction between the $S = \frac{1}{2}$ cations is not likely to be uniform in all the three dimensions; the interaction between the transition-metal atoms would be more pronounced in the (130) planes (the MoO_6 octahedra are connected by edges in these planes) than in the direction perpendicular to these planes. Considering that the ordering of the transition-metal atoms in the parent brannerite sheets[9,10] is most probably retained in the (130) planes of the product $LiVMoO_5$ phases, one would

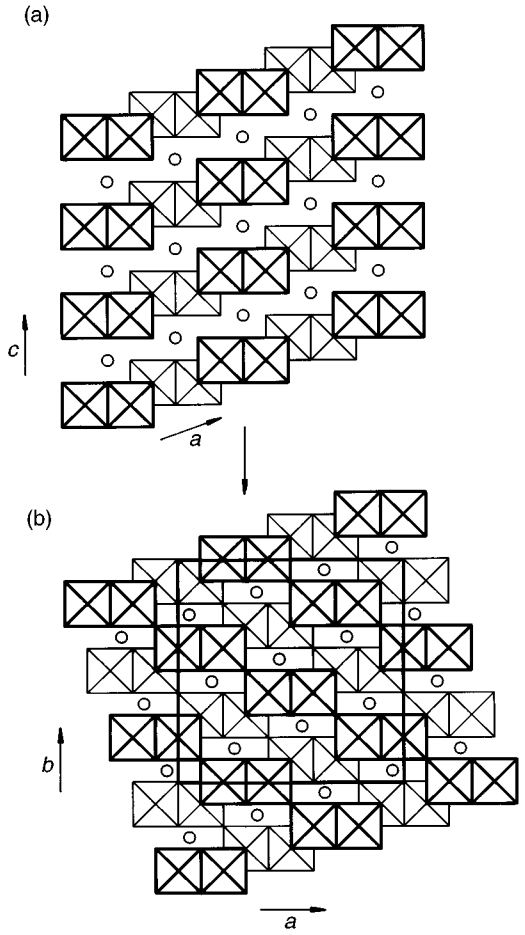

Fig. 4 Idealized representation of the structural transformation of $LiVMoO_6$ (a) to $LiVMoO_5$ (b). Open circles represent the Li atoms.

expect quasi-two-dimensional electronic properties for these materials.

We show the electrical resistivity data for $LiVMO_5$ in Fig. 5 and 6. We see that the tungsten compound is semiconducting (Fig. 5), having a small activation energy (0.005 eV) in the 100–20 K region. The molybdenum compound ($LiVMoO_{5.04}$), on the other hand, is metallic down to 230 K, below which it shows a metal–semiconductor–metal transition [Fig. 6(a)]. The resistivity decreases with temperature down to 240 K; below 230 K it increases showing a maximum at 120 K. The resistivity below 120 K again decreases down to 20 K. This resistivity behaviour is reminiscent of quasi-low-dimensional molybdenum oxides, $A_xMo_6O_{17}$ (A = Na, K, Tl) which show a CDW transition.[4] The electrical resistivity of another sample having

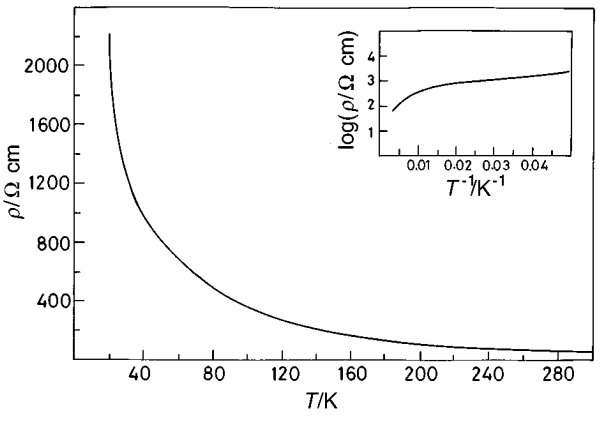

Fig. 5 Plot of resistivity (ρ) *vs.* temperature (T) for $LiVWO_5$. The inset shows the plot of $\log(\rho)$ *vs.* T^{-1}.

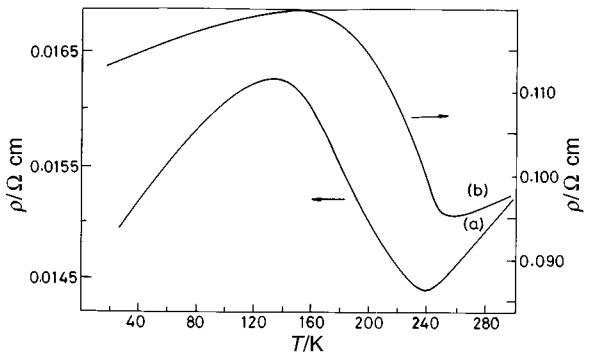

Fig. 6 Plots of resistivity (ρ) *vs.* temperature (T) for (a) $LiVMoO_{5.04}$ and (b) $LiVMoO_{5.08}$

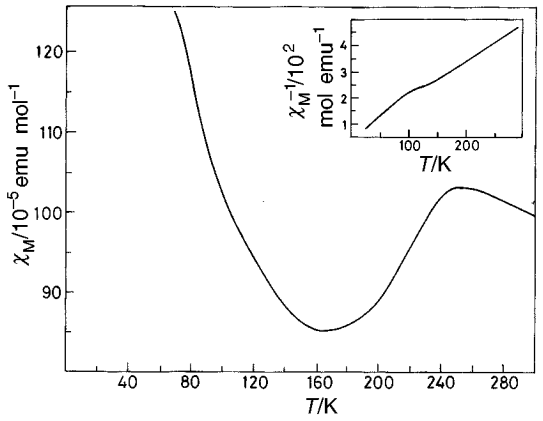

Fig. 7 Plot of molar magnetic susceptibility (χ_M) *vs.* temperature (T) for $LiVMoO_{5.04}$. The inset shows χ_M^{-1} *vs.* T for $LiVWO_5$.

the composition $LiVMoO_{5.08}$ [Fig. 6(b)] also shows similar behaviour, although there is an increase in both the CDW transition temperature (250 K) and the resistivity. The increase in resistivity of this phase could possibly be attributed to the higher oxygen content (and hence a smaller charge-carrier concentration) than $LiVMoO_{5.04}$. The specific heat measurements also support the existence of a CDW transition showing a broad maximum in the region 210–270 K.

Magnetic susceptibility data (Fig. 7) of $LiVMoO_{5.04}$ corroborate the resistivity behaviour, showing a characteristic drop in the susceptibility around the transition temperature (230 K). Similar susceptibility data have been reported for $A_xMo_6O_{17}$ oxides.[4] The drop in the susceptibility and the increase in the resistivity at the CDW transition have been attributed[2] to a decrease in the density of states at the Fermi level (E_F) signaling the onset of a CDW transition. $LiVWO_5$, on the other hand, shows Curie–Weiss paramagnetic behaviour (Fig. 7 inset) and the effective magnetic moment obtained from the χ_M^{-1} *vs* T plot (300–150 K) is 2.41 μ_B, while the value calculated from the spin-only formula for $V^{IV}:3d^1$ and $W^V:5d^1$ configurations is 2.45 μ_B. At temperatures below 150 K, there is a change in the slope showing a slight enhancement of the susceptibility. The Curie–Weiss behaviour of the tungsten compound is consistent with its semiconducting nature, indicating that $V^{IV}:3d^1$ and $W^V:5d^1$ electrons are localized.

The electrical and magnetic properties of $LiVMO_5$ (M = Mo, W) show that the electronic interaction between the $S=\frac{1}{2}$ atoms, $V^{IV}:3d^1$ and $Mo^V:4d^1$, in $LiVMoO_5$ produces itinerant states that support a CDW instability, while the interaction between $V^{IV}:3d^1$ and $W^V:5d^1$ in the isotypic $LiVWO_5$ does not produce itinerant states and the associated electronic instability at low temperatures. While the present work has shown the possibility of a CDW instability in a new oxide containing two different $S=\frac{1}{2}$ atoms, *viz.* $V^{IV}:3d^1$ and $Mo^V:4d^1$, further work is essential to establish the detailed structure and electronic properties of this oxide.

Conclusions

We have synthesized two new oxides, $LiVMO_5$ (M = Mo, W), containing $S=\frac{1}{2}$ cations which belong to $3d^1$ and $4d^1/5d^1$ series, by topotactic reduction of the brannerites $LiVMO_6$ (M = Mo, W). The orthorhombic structure of $LiVMO_5$, derived from the parent layered $LiVMO_6$, is quasi-two-dimensional, showing interesting electronic properties. While $LiVWO_5$ is paramagnetic and semiconducting, $LiVMoO_5$ is metallic showing indications of a CDW instability around 230 K.

We thank Professor C. N. R. Rao, F.R.S. for encouragement and support and the Indo-French Centre for the Promotion of Advanced Research, New Delhi, for financial support. N. S. P. B. thanks the Council of Scientific and Industrial Research, New Delhi, for the award of a senior research fellowship.

References

1 F. J. Morin, *Phys. Rev. Lett.*, 1959, **3**, 34.
2 J. B. Goodenough, *Phys. Rev.*, 1960, **117**, 1442.
3 R. M. Wentzcovitch, W. W. Schulz and P. B. Allen, *Phys. Rev. Lett.*, 1994, **72**, 3389.
4 *Low-Dimensional Electronic Properties of Molybdenum Bronzes and Oxides*, ed. C. Schlenker, Kluwer, Dordrecht, 1989.
5 E. Canadell and M-H. Whangbo, *Chem. Rev.*, 1991, **91**, 965.
6 E. Dagotto and T. M. Rice, *Science*, 1996, **271**, 618.
7 J. G. Bednorz and K. A. Müller, *Z. Phys. B*, 1986, **64**, 189.
8 *Chemistry of Superconductor Materials*, ed. T. A. Vanderah, Noyes Publications, Park Ridge, New Jersey, 1992.
9 J. Galy, J. Darriet and B. Darriet, *C. R. Acad. Sci. Paris*, 1967, **264**, 1477.
10 J. Galy, G. Meunier, J. Senegas and P. Hagenmuller, *J. Inorg. Nucl. Chem.*, 1971, **33**, 2403.
11 R. Ruh and A. D. Wadsley, *Acta Crystallogr.*, 1966, **21**, 974.
12 W. Lasocha and K. Lewinski, *J. Appl. Crystallogr.*, 1994, **27**, 437.
13 A. F. Wells, *Philos. Trans. R. Soc., London A*, 1984, **312**, 553.

Paper 6/06392F; *Received* 17*th September*, 1996